Environmental Science Nano

ROYAL SOCIETY OF CHEMISTRY

PAPER

View Article Online
View Journal | View Issue

Cite this: *Environ. Sci.: Nano*, 2021, **8**, 1690

Mechanisms and effects of zinc oxide nanoparticle transformations on toxicity to zebrafish embryos†

Gyudong Lee, [a] Byongcheun Lee[b] and Ki-Tae Kim *[a]

The effect of transformations on the toxicity of zinc oxide nanoparticles (ZnO NPs) and the underlying mechanisms are unclear, limiting our understanding of the realistic impacts of ZnO NPs in the environment. Three kinds of ZnO NP transformations were induced through interaction with sulfur (sulfidation) and phosphate (phosphation) and association with hydrous ferric oxide (Zn–FeOOH). Pristine and transformed ZnO NPs were characterized using X-ray diffraction and transmission electron microscopy. Changes in toxicity as a result of transformation were evaluated using an embryonic zebrafish assay. Toxicity was reduced in descending order by phosphation, sulfidation, and Zn–FeOOH with increasing molar ratios of S/Zn, PO_4/Zn, and Fe/Zn, respectively. Reduced toxicity correlated well with the zinc concentration and addition of ethylenediaminetetraacetic acid completely eliminated the toxicity, indicating that the remaining zinc ions in bulk solution were responsible for the toxicity of transformed ZnO NPs. The maximum toxicity reduction was observed after phosphation, attributable to the inhibition of zinc release by phosphates rapidly enclosing ZnO NPs. Zn–FeOOH does not effectively reduce the zinc concentration because no significant morphological changes occur during the transformation. We demonstrated that transformations modified the physicochemical properties of ZnO NPs, modulating their ability to reduce zinc ions, and governing toxicity to zebrafish embryos.

Received 2nd April 2021,
Accepted 28th April 2021

DOI: 10.1039/d1en00305d

rsc.li/es-nano

Environmental significance

Zinc oxide nanoparticles (ZnO NPs) undergo transformations in wastewater treatment plants and water environments, resulting in changes in physicochemical properties. Thus, to accurately evaluate the ecological toxicity of ZnO NPs, the effects of transformations and underlying mechanisms of toxicity must be considered. The relative toxicity changes of three types of ZnO NP transformations are compared using zebrafish embryos. A reduction in toxicity occurs in a descending order of phosphate-, sulfide-, and FeOOH-transformed ZnO NPs. Toxicity reduction correlates well with zinc concentration, indicating that altered physicochemical properties as a result of transformation determine the ability to reduce zinc ions and that the remaining zinc ions are responsible for the degree of toxicity reduction caused by the transformation.

Introduction

Zinc oxide nanoparticles (ZnO NPs) are used in a wide range of industrial and personal care products;[1–3] the unique antibacterial and anticancer properties of ZnO NPs have expanded their applications into the biomedical field.[4,5] Accordingly, concerns have been raised over the increasing production and subsequent release of ZnO NPs into aquatic environments, which poses a toxicity risk for aquatic organisms.[6] Indeed, among engineered nanomaterials (ENMs), ZnO NPs have high potential to cause aquatic toxicity due to the toxic zinc ions embedded within them.[7–9] Previous studies have demonstrated that environmental transformations can modify the physicochemical properties of ZnO NPs; thus, when evaluating ecological toxicity, transformations should be considered in addition to pristine ZnO NPs to gain an environmentally-relevant understanding of their effects.[10–12] However, compared to characterization of altered physicochemical properties, few studies have reported changes in toxicity due to transformations.

ZnO NPs readily undergo transformations mediated by ions and biosolids present in wastewater treatment plants

[a] *Department of Environmental Engineering, Seoul National University of Science and Technology, Seoul, 01811, Republic of Korea. E-mail: rbehd8024@gmail.com, ktkim@seoultech.ac.kr; Fax: +82 2 970 5776; Tel: +82 2 970 6642*
[b] *Risk Assessment Division, National Institute of Environmental Research, Incheon, 22689, Republic of Korea*

† Electronic supplementary information (ESI) available: Neoformation level of sulfidation and phosphation (Table S1), percentage of malformation in zebrafish embryos exposed to three type of transformed zinc oxide nanoparticles (ZnO NPs) (Table S2), physicochemical properties and embryonic toxicity of pristine ZnO NPs, and zinc concentration in the bulk solution (Fig. S1), EDX results of transformed ZnO NPs at various molar ratios (Fig. S2), images for malformed zebrafish embryos exposed to transformed ZnO NPs (Fig. S3), embryonic toxicity of solutions in which each sulfur, phosphate, and hydrous ferric oxide were added to zinc chloride ($ZnCl_2$) (Fig. S4), correlation between internal concentration of zinc and toxicity (Fig. S5). See DOI: 10.1039/d1en00305d

(WWTPs).[13–15] Typically, ZnO NPs are often environmentally transformed through interactions with sulfide ions (sulfidation) and phosphate ions (phosphation), or association with hydrous ferric oxide (Zn–FeOOH).[13–18] Previous studies describe changes in physicochemical properties, resulting from transformations and the influence of these alterations on toxicity. Sulfidation of ZnO reduces toxicity by inducing the exchange of oxygen with sulfur; the ZnS formed has low solubility, inhibiting the release of zinc ions.[16] In comparison with pristine ZnO NPs, several studies have demonstrated that sulfidation of ZnO NPs reduces toxicity to nematodes, earthworms, and epibenthic amphipods.[19–21] The observed reduction in toxicity with sulfidation appears to be independent of the ZnO NP morphology. Recently, sulfidation of urchin-like ZnO NPs reduced toxicity to *Escherichia coli*.[22] Conversely, phosphation is known to increase cytotoxicity[23] and toxicity to the benthic invertebrate, *Hyalella azteca*.[21] However, the effect of phosphation on the toxicity of ZnO to higher aquatic organisms such as fish has not been reported. The phosphation process involves the transformation or degradation of ZnO by phosphate ions to form zinc phosphate ($Zn_3(PO_4)_2$) crystallites.[17,18] Additionally, the association of ZnO NPs with FeOOH induces the formation of inner-sphere surface complexes of Zn–O–Fe,[24] resulting in zinc-sorbed or -substituted FeOOH.[13–15] To our knowledge, the effect of Zn–FeOOH on toxicity has not been investigated.

Many toxicological studies have utilized zebrafish embryos to investigate the toxicity of ENMs.[25–27] A resource-efficient toxicity assessment using zebrafish is feasible due to their small embryo size and high fecundity, and only a small volume of test solution is needed. In addition, the chorion can be removed, and zebrafish embryos can develop for 5–6 days without noticeable malformations in solutions with low ionic strength, including Milli-Q water. These characteristics of zebrafish embryonic assays are specified for nanotoxicology; when assessing the toxicity of ENMs, such advantages prevent secondary agglomeration during testing. Applying these distinctive traits to assess the toxicity of silver nanoparticles (AgNPs), a previous study demonstrated that polyvinylpyrrolidone-coated or smaller-sized AgNPs are more toxic than citrate-coated or larger-sized AgNPs in a controlled ionic environment.[28] Therefore, we conjecture that implementing these experimental conditions to perform a comparative analysis of transformed ZnO NP toxicity will be effective, producing more reliable and accurate toxicological data by reflecting the intact physicochemical properties modified by the transformations.

We induced three types of ZnO NP transformation (*i.e.*, sulfidation, phosphation, and Zn–FeOOH) as a function of different molar ratios of S/Zn, PO_4/Zn, and Fe/Zn, respectively. We characterized the changes in the structural properties, morphologies, and hydrodynamic diameters with zeta potentials of each transformed ZnO NP in comparison to pristine ZnO NPs. A zebrafish embryonic toxicity assay was then conducted; the introduction of a test model system is useful for comparative analysis of the relative extent of toxicity change induced by the transformation of ZnO NPs. In addition, we quantified the zinc concentrations in each bulk solution of transformed ZnO NPs to elucidate the mechanism underlying the toxicity changes. Toxicity testing was repeated after zinc ions were eliminated by adding ethylenediaminetetraacetic acid (EDTA), a chelating agent.

Experimental

Chemicals

ZnO nanopowder dispersed in water (CAS: 1314-13-2, >99.5% purity) was purchased from US Research Nanomaterials, Inc. (Houston, TX, USA). According to the information provided by the manufacturer, the ZnO NPs are spherical in shape and 30–40 nm in size. Sodium sulfide pentahydrate ($Na_2S{\cdot}5H_2O$, CAS: 1313-83-3, ≥98.0% purity) was purchased from Daejung Chemicals & Metals (Shiheung, South Korea). Sodium phosphate monobasic (H_2NaPO_4, CAS: 7558-80-7, ≥99.0% purity) and ethylenediaminetetraacetic acid disodium salt dihydrate ($Na_2H_2EDTA{\cdot}2H_2O$, CAS: 6381-92-6, 99.0–101.0% purity) were purchased from Sigma-Aldrich (St Louis, USA). Sodium hydroxide (NaOH, CAS: 1310-73-2, ≥99.0% purity) and iron(III) chloride ($FeCl_3$, CAS: 7705-08-0, ≥97.0% purity) were purchased from Duksan Pure Chemical (Ansan, South Korea).

Transformation of ZnO NPs

Sulfide, phosphate, and hydrous ferric oxide dissolved in Milli-Q water were added to 50 mg L^{-1} ZnO NPs to induce transformation. Desired S/Zn and PO_4/Zn molar ratios of 0.484, 0.968, and 1.936 were used for sulfidation and phosphation. The molar ratios used for sulfidation[16] were adjusted for phosphation. The molar ratio of PO_4/Zn instead of P/Zn was used to better express the relative toxicity changes. Hydrous ferric oxide was prepared by adding NaOH to $FeCl_3$ solution.[29] The molar ratio of Fe/Na was adjusted to one. The $FeCl_3$ solution color changed from yellow to orange after adding NaOH. Zn–FeOOH was prepared with Fe/Zn molar ratios of 0.484, 0.968, 1.936, 4.84, 9.68, and 19.36. The pH values of all the samples were adjusted to 6.5–7.5 using HCl and NaOH. After preparation, the transformed ZnO NPs were incubated at room temperature for 12 h, before characterization and toxicity testing.

Characterization of pristine and transformed ZnO NPs

The structural composition of the pristine and transformed ZnO NPs was characterized using X-ray diffraction (XRD) (Bruker DE/D8 Advance, Bruker, Germany). The concentration was optimized to 2000 mg L^{-1} for XRD analysis in the preliminary experiments. After the solution was centrifuged at 15 000 rpm for 30 min, the dried samples were prepared by freezing at −90 °C using a freeze dryer. The XRD peaks were collected with continuous scanning in the 2θ range of 10–80°. The peaks generated by sulfidation,

phosphation, and Zn–FeOOH were compared with those of the pristine ZnO NPs and molecules composed of zinc with sulfur, phosphate, and FeOOH: ZnS, $Zn_3(PO_4)_2$, and ZnFeOOH. The hydrodynamic diameters and zeta potentials of the transformed ZnO NPs were measured using a particle size analyzer (ELS-Z, Otsuka Electronics, Japan). The values were averaged from the three measurements for each sample. The morphology of the pristine ZnO NPs and transformed ZnO NPs was measured using a transmission electron microscope (TEM) (JEM-2010, JEOL, Japan). Changes in the structural and elemental composition of the transformed ZnO NPs were measured using a scanning transmission electron microscope (STEM) (NEO ARM, JEOL, Japan) with surface area electron diffraction (SAED) and energy dispersive X-ray spectroscopy (EDX), respectively. The obtained images and data were then compared with the results of the pristine ZnO NPs. Characterization of the pristine ZnO NPs was conducted at a concentration of 50 mg L^{-1} diluted with Milli-Q water.

Zebrafish culture and embryonic toxicity testing

Wild-type (5D strain) adult zebrafish (*Danio rerio*) cultures have been maintained at 28 °C ± 2 °C and 14/10 h light/dark cycle conditions in a flow-through system (Zebtec, Tecniplast, Italy) since 2014. Healthy mature zebrafish were paired in spawning tanks the day before experiments. Healthy embryos at the same developmental stage were sorted using an optical microscope (Nikon, Japan). The collected embryos were maintained at 28 °C in an incubator in embryo rearing E2 media. To prepare the embryos for toxicity testing, the chorion was removed at 4 h post-fertilization (hpf) using 200 μg ml^{-1} pronase (Sigma-Aldrich, St. Louis, USA) in E2 media, following the methods previously conducted in our laboratory.[30] In a 96-well plate, individual dechorionated embryos were transferred into wells containing 100 μL of test solution. Twenty-four dechorionated embryos per each concentration were exposed from 6 to 120 hpf. Milli-Q water, which was used to prepare the transformed ZnO NPs, served as a negative control in each replicate. Toxicity testing was performed in triplicate. The plates were covered with aluminum foil to avoid photodegradation and incubated at 28 °C without renewal of the test solutions. The incidence of embryonic mortality was recorded at 120 hpf. The toxicity patterns of the transformed ZnO NPs were compared with those in the $ZnCl_2$ solution to which we added sulfur, phosphate, and hydrous ferric oxide molar ratios corresponding to those used for ZnO NP transformations. The concentration of $ZnCl_2$ was fixed at 84 mg L^{-1}, which corresponds to the zinc molar concentration in 50 mg L^{-1} ZnO NPs. All animal procedures were performed in accordance with the Guidelines for Care and Use of Laboratory Animals of Seoul National University of Science and Technology and approved by the Animal Ethics Committee of Seoul National University of Science and Technology (approval#: 2019-0002).

The effect of zinc ions on toxicity changes

To investigate the effect of zinc ions on toxicity changes, we measured the zinc concentration in bulk solutions of 50 mg L^{-1} pristine and transformed ZnO NPs using inductively coupled plasma atomic emission spectroscopy (ICP-OES) (5110 SVDV, Agilent, Singapore). The prepared solution was incubated at room temperature for 12 h (the same duration as that for toxicity testing) and then centrifuged at 10 000 *g* for 30 min prior to analysis. The zinc concentration in the pristine ZnO NP bulk solution was measured seven times over 120 h. The reported concentrations are the average of three measurements for each sample. In addition, we examined the effect of zinc ions on toxicity using biological toxicity testing. We added EDTA to the bulk solutions of pristine and transformed ZnO NPs to eliminate the zinc ions. The chelating agent was added just after each transformed ZnO NP solution was prepared and the EDTA/Zn molar ratio was adjusted to one. Finally, an additional embryonic toxicity test was conducted under the same conditions (24 dechorionated embryos, 6–120 hpf exposure duration, three replicates).

Statistics

Embryonic mortality and zinc concentrations were presented as mean ± standard deviation using SigmaPlot 13 (Systat Software Inc., San Jose, CA). The toxicological values for lethal concentrations were calculated with 95% confidence interval (CI) using IBM SPSS Statistics 25. Using a one-way analysis of variance (ANOVA) followed by Tukey's *post-hoc* for multiple comparisons, significant differences in embryonic mortality were defined as p-values < 0.05.

Results and discussion

Characterization of pristine and transformed ZnO NPs

First, we verified the physicochemical properties of the pristine ZnO NPs. TEM analysis confirmed that the ZnO NPs were spherical with an average particle size of 30–40 nm (Fig. S1A†). The pristine ZnO NPs involved the zinc and oxygen and had the crystalline structure in EDX and SAED analysis, respectively (Fig. S1†). XRD analysis revealed sharp peaks at approximately 30° and between 50° and 80°, indicating that the ZnO NPs are in the form of crystalline zincite (Fig. S1D,† Fig. 1). The hydrodynamic diameter and zeta potential were 0.98 ± 0.18 μm and −33.20 ± 3.56 mV, respectively (Table 1).

The surface chemical compositions of the three transformed ZnO NPs were characterized using EDX, SAED, and XRD with increasing molar ratios of S/Zn, PO_4/Zn, and Fe/Zn; the morphologies were imaged using TEM (Fig. 2). The neoformation level of sulfidation and phosphation was obtained using the XRD peak intensities (Table S1†). Overall,

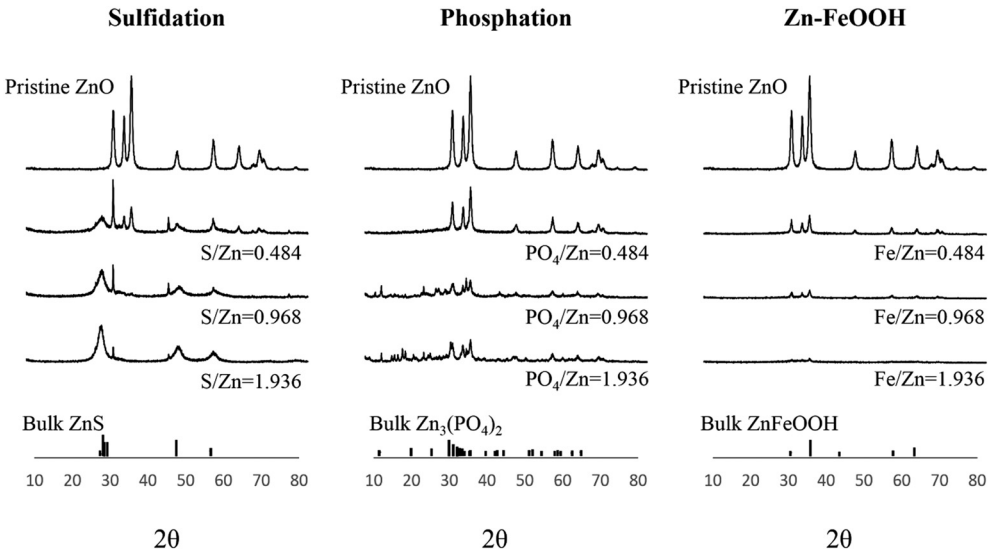

Fig. 1 X-ray diffraction (XRD) analysis of the surface chemical composition of the three kinds of transformed zinc oxide nanoparticles (ZnO NPs). XRD spectra of sulfidation, phosphation, and Zn–FeOOH. XRD peaks of the pristine ZnO NPs are shown in the first line and XRD peaks of the zinc ionic molecules (ZnS, $Zn_3(PO_4)_2$, and ZnFeOOH) are shown in the last line, respectively.

the analyzed features illustrate the characteristics of the transformed ZnO NPs, which depends on the ions and biosolids that interact with the pristine ZnO NPs. In EDX analysis (Fig. S2†), each transformed ZnO NP basically involved the zinc and oxygen observed in the pristine ZnO NPs and had the respective elements (sulfur for sulfidation, phosphorus for phosphation, and iron for Zn–FeOOH). The peak intensities for these elements increased with increasing molar ratios. In SAED analysis (Fig. 3), we found that the crystalline structure was maintained in sulfidation and Zn–FeOOH whereas the white spots in the circle disappeared in phosphation, indicating the formation of an amorphous structure by phosphation. In particular, diffraction rings in the circle were observed instead of white spots in sulfidation, suggesting that a polycrystalline structure was formed after sulfidation.[31] In addition, we quantitatively analyzed the neoformation level by dividing the XRD peak intensity at 29° by that at 36° (P_{29}/P_{36}) for sulfidation, and by dividing the XRD peak intensity at 31° by that at 36° (P_{31}/P_{36}) for phosphation. As a result, the neoformation observed in sulfidation and phosphation increased with increasing molar ratios of S/Zn and PO_4/Zn, and no neoformation was observed in Zn–FeOOH (Table S1†).

Table 1 Hydrodynamic diameters and zeta potentials of pristine zinc oxide nanoparticles (ZnO NPs) and the three kinds of transformed ZnO NPs

Type of ZnO NPs	Molar ratios	Hydrodynamic diameter (μm)	Zeta potential (mV)
Pristine ZnO NPs	—	0.98 ± 0.18	−33.20 ± 3.56
Sulfidation (S/Zn)	0.484	9.55 ± 2.07	−2.03 ± 4.06
	0.968	6.50 ± 2.05	−14.18 ± 0.72
	1.936	5.17 ± 0.56	−41.55 ± 0.61
Phosphation (PO_4/Zn)	0.484	2.65 ± 0.22	−34.00 ± 1.84
	0.968	1.11 ± 0.17	−35.76 ± 2.39
	1.936	5.08 ± 0.64	−34.71 ± 0.61
Zn–FeOOH (Fe/Zn)	0.484	14.79 ± 1.87	−14.48 ± 6.68
	0.968	10.89 ± 0.990	4.09 ± 3.96
	1.936	15.97 ± 1.400	9.84 ± 3.18

The XRD peak pattern observed after sulfidation was consistent with previous studies.[16,20,32] New XRD peaks were generated at around 30°, which were not observed in the pristine ZnO NPs, suggesting the formation of ZnS. The newly-generated representative peaks became apparent with increasing S/Zn molar ratios and the intensity of the peaks of the pristine ZnO NPs continuously decreased, indicating that sulfidation progressed with increasing concentrations of sulfur ions.[16,32] Direct comparison of the XRD results for phosphation was difficult because the PO_4/Zn molar ratios were varied across previous studies; however, the XRD peaks observed after phosphation were comparable to those in a previous study.[17] The intensity of the peaks of the pristine ZnO NPs was reduced with increasing PO_4/Zn molar ratios, and new XRD peaks were generated with a PO_4/Zn molar ratio of 1.936. Newly-generated XRD peaks between 10° and 40° indicate the formation of crystalline $Zn_3(PO_4)_2$ (*i.e.*, hopeite). These peaks became apparent at PO_4/Zn molar ratios higher than 0.484. A previous study reported the coexistence of both amorphous and crystalline forms as a result of phosphation between pH 6 and 8.[32,33] Amorphous forms that could not be discerned by XRD signals were detected at low PO_4/Zn ratios in TEM analysis, which was confirmed by disappearance of white spots in SAED patterns.

In contrast to sulfidation and phosphation, Zn–FeOOH did not generate new XRD peaks. Instead, the peaks of the pristine ZnO NPs decreased or disappeared with increasing Fe/Zn molar ratios. However, unlike phosphation, this result does not imply the formation of amorphous particles; no morphological changes were observed in the TEM images

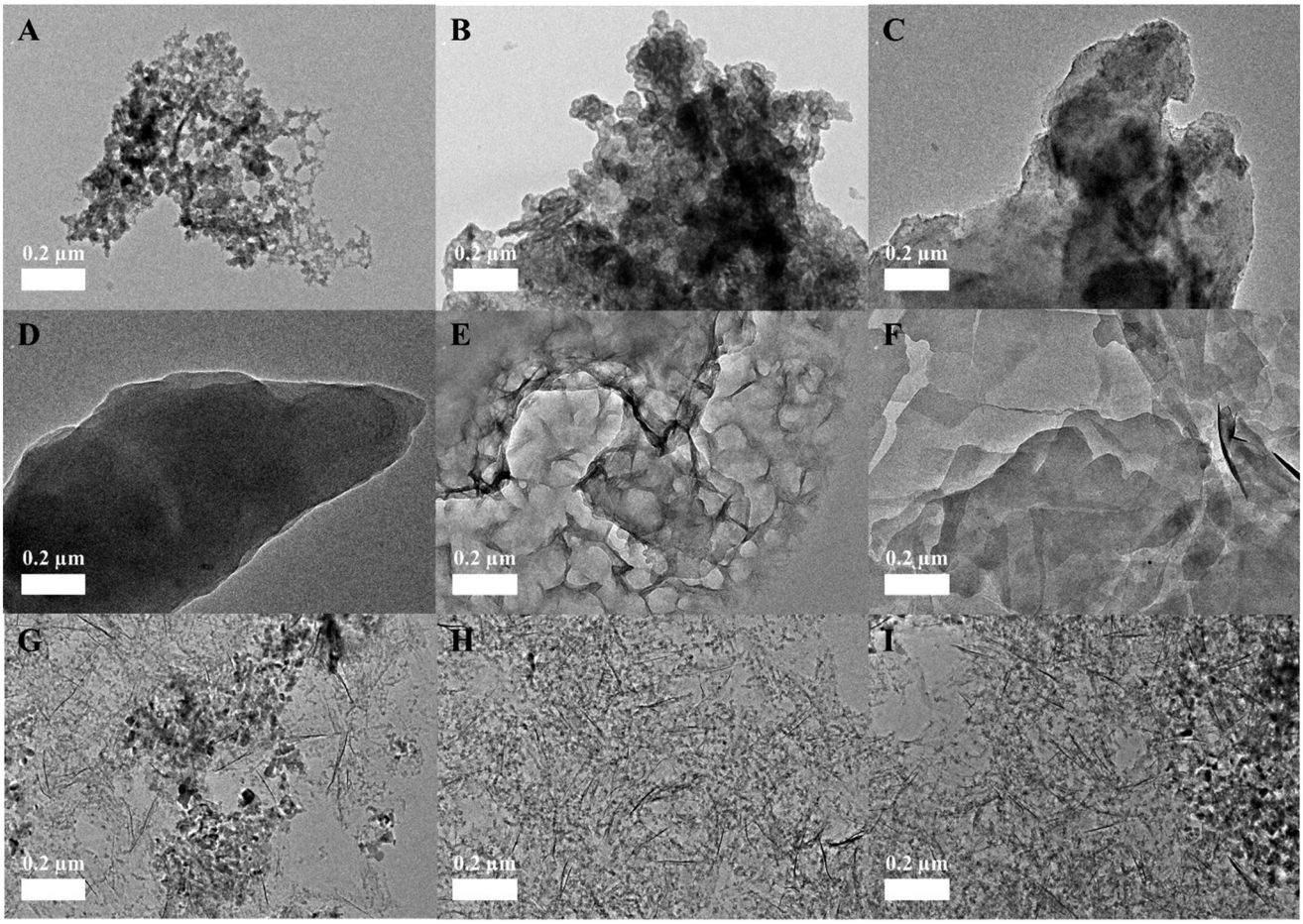

Fig. 2 TEM images of sulfidation, phosphation, and Zn–FeOOH: (A) S/Zn = 0.484; (B) S/Zn = 0.968; (C) S/Zn = 1.936; (D) PO_4/Zn = 0.484; (E) PO_4/Zn = 0.968; (F) PO_4/Zn = 1.936; (G) Fe/Zn = 0.484; (H) Fe/Zn = 0.968; (I) Fe/Zn = 1.936.

and SAED analysis confirmed that the crystalline structure was maintained in Fe–ZnOOH at all Fe/Zn ratios.

In addition, the analytical hydrodynamic diameter and zeta-potential results illustrate individually-differentiated characteristics of each transformed ZnO NP (Table 1). Compared to the pristine ZnO NPs, the hydrodynamic diameters dramatically increased with sulfidation after adding low concentrations of sulfide ions, then decreased as the S/Zn molar ratios increased. Simultaneously, the zeta-potentials were significantly lower at low S/Zn molar ratios than those measured in the pristine ZnO NPs and became much greater as the molar ratio increased. This opposing trend between the hydrodynamic diameter and zeta-potential is generally acceptable; sulfur replacement on the surface increases the zeta-potential, which in turn stabilizes the particles, alleviating agglomeration. Interestingly, no abrupt change in the zeta-potential was observed with phosphation at any PO_4/Zn molar ratio compared to the pristine ZnO NPs, and the hydrodynamic diameters increased only at the highest molar ratio. Thus, phosphate ions do not appear to affect zeta-potential. Among the three transformed ZnO NPs, the hydrodynamic diameters were greatest in Zn–FeOOH and an unordered zeta-potential pattern was observed with varying Fe/Zn molar ratios.

Embryonic toxicity of the transformed ZnO NPs

We first evaluated the embryonic toxicity of the pristine ZnO NPs in order to investigate the effect of transformations on toxicity changes. Mortality increased in a concentration-dependent manner (Fig. S1E†). Exposure to the pristine ZnO NPs also caused malformations such as yolk sac edema, pericardial edema, spinal kyphosis, and tail malformation (Fig. S1F†); however, malformation incidence was not concentration dependent, and no specific malformation was observed consistently. At 50 mg L^{-1}, 100% mortality was observed and LC_{50} was calculated as 13.8 mg L^{-1} (11.6–16.2 mg L^{-1}, 95% CI). The physicochemical properties of the transformed ZnO NPs could be altered when they pass through the chorion, which is composed of proteins, and the presence of a chorion could lead to indirect secondary effects due to impermeability.[34] Therefore, dechorionation is favorable for the purpose of this study. However, no difference in toxicity was observed in the absence and presence of chorion; the obtained LC_{50} was 16.4 mg L^{-1}

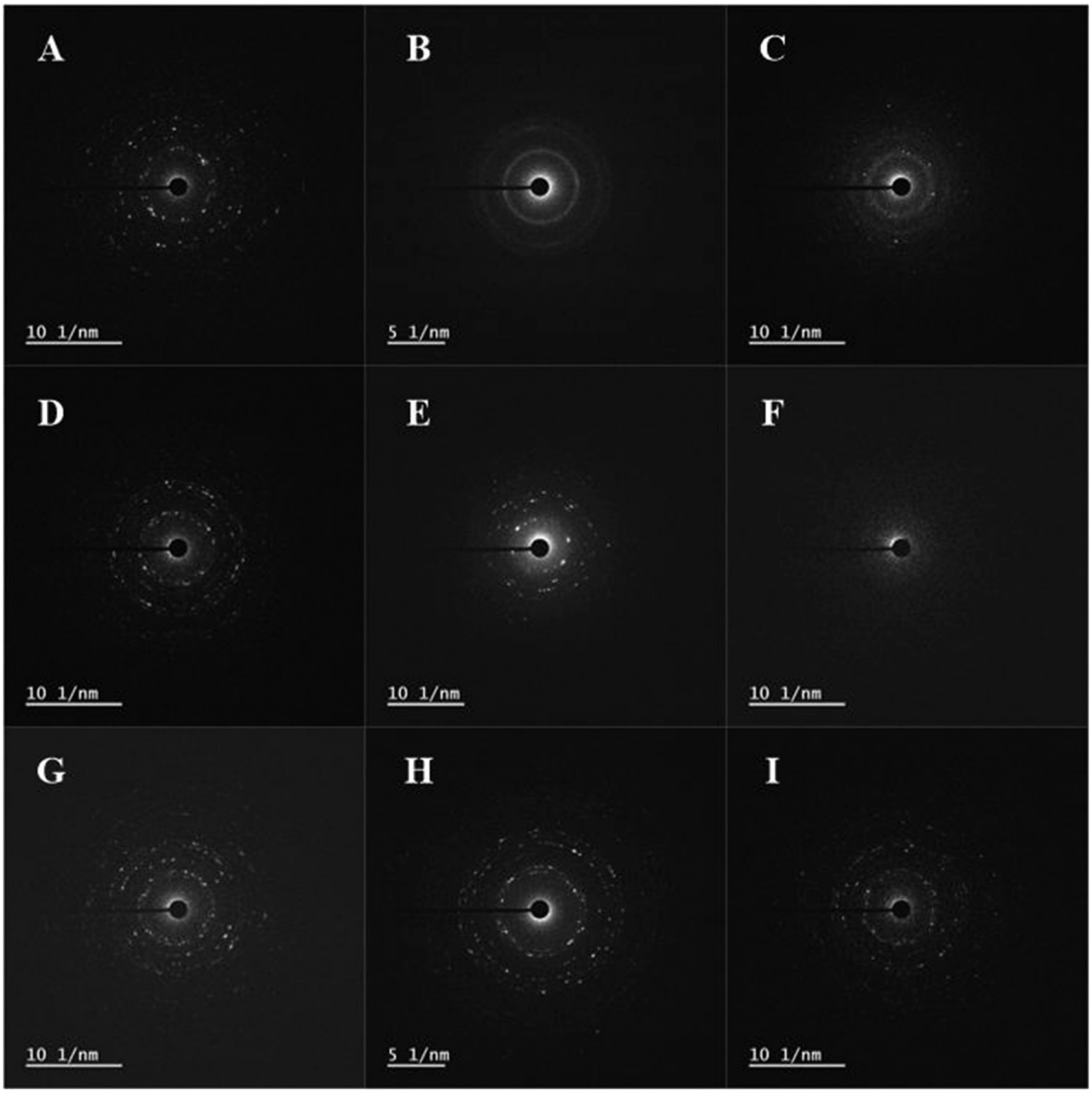

Fig. 3 SAED patterns of sulfidation, phosphation, and Zn–FeOOH: (A) S/Zn = 0.484; (B) S/Zn = 0.968; (C) S/Zn = 1.936; (D) PO_4/Zn = 0.484; (E) PO_4/Zn = 0.968; (F) PO_4/Zn = 1.936; (G) Fe/Zn = 0.484; (H) Fe/Zn = 0.968; (I) Fe/Zn = 1.936.

(13.5–19.2 mg L^{-1}, 95% CI) in chorionated embryos, which was similar to the previously reported value (*i.e.*, 11.9 mg L^{-1} for 43 nm ZnO NPs).[35]

Next, we compared the embryonic toxicity of the three kinds of transformed ZnO NPs. Compared to the pristine ZnO NPs, the overall toxicity to zebrafish embryos was reduced by all three transformations (Fig. 4). To clarify, only embryonic mortality was considered in the analysis; the incidence of malformation in groups exposed to each transformed ZnO NP and images of malformed larvae are shown in Table S2 and Fig. S3.† The patterns of toxicity reduction were notably varied. A significant reduction in toxicity was observed at molar ratios of 0.968 and 1.936 with sulfidation. Ma *et al.* (2013) estimated the ratio between ZnO and ZnS NPs at different S/Zn molar ratios and reported partial sulfidation at S/Zn initial molar ratios of less than 2.[16] Thus, toxicity may be reflective of partial sulfidation. Compared to sulfidation, toxicity was significantly reduced in phosphation at lower molar ratios. Conversely, with Zn–FeOOH, no reduction in toxicity was observed at the equivalent Fe/Zn molar ratios (*i.e.*, 0.484, 0.968, and 1.936). Interestingly, we observed a significant reduction in toxicity at much higher molar ratios (*i.e.*, 9.68 and 19.36).

This study is the first to compare the degree of change in relative toxicity among three types of ZnO NP transformations using one toxicity model, zebrafish embryos. We demonstrated that embryonic toxicity was reduced in a descending order phosphation > sulfidation > Zn–FeOOH. Phosphation is more effective in reducing the toxicity of ZnO NPs than sulfidation, which is seen more clearly when considering the molar ratio of PO_4/Zn. Recently, Poynton *et al.* (2019) compared the effects of two transformations on

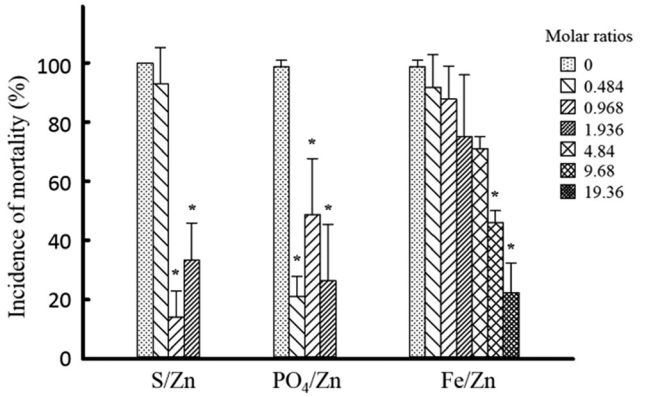

Fig. 4 The percent incidence of embryonic mortality in zebrafishes exposed to zinc oxide nanoparticles (ZnO NPs) transformed by sulfidation, phosphation, and Zn–FeOOH at different molar ratios. Three replicates of 24 embryos were exposed to each transformed ZnO NP from 6 to 120 h post-fertilization. The values are presented as mean ± standard deviation (SD). Significant differences ($p < 0.05$) between the toxicity of 50 mg L^{-1} pristine ZnO NPs and toxicity of groups treated with transformed ZnO NPs are marked by (*).

toxicity using epibenthic crustacean *Hyalella azteca* and reported that sulfidation reduces toxicity while phosphation enhances toxicity.[21] In contrast, both sulfidation and phosphation reduced toxicity to *Caenorhabditis elegans*.[19] In our study, we observed reduced toxicity of ZnO NPs to embryonic zebrafish with all three transformations. Therefore, changes in toxicity are dependent on the type of transformation and the test species. As described in the Experimental section, toxicity testing was performed without re-dispersion of the transformed ZnO NPs in test media. Since the transformation of ZnO NPs can be affected by ions such as calcium, magnesium, and even phosphate[12,17] (which was used to induce phosphation in this study), the ionic composition of the test media could confound the comparative analysis of toxicity changes as a result of transformation. Toxicity testing should be conducted in a controlled ionic environment to effectively reflect the unvarnished characteristics of the transformed ZnO NPs. However, environmental factors in the transformation process and subsequent toxicity change, such as natural organic matter, light, and various ionic strengths, should be further considered to reflect environmentally relevant conditions.

Although several studies have expressed that environmental transformation alters the fate and impact of ENMs and should be taken into consideration,[10,12] few have reported toxicity changes as a result of transformation, particularly in ZnO NPs. Most sulfidation studies have investigated AgNPs, reporting toxicity reduction toward various test species including bacteria, fish, and nematodes.[36–38] We observed reduced ZnO NP toxicity to zebrafish with sulfidation, which is consistent with other studies using nematodes, earthworms, and epibenthic amphipods.[19–21] However, another study reported that sulfidation enhances the toxicity of copper oxide nanoparticles to medaka.[39] Furthermore, we discovered that phosphation and Zn–FeOOH reduced the toxicity of ZnO NPs to zebrafish embryos; however, few studies have reported the effects of phosphation and Zn–FeOOH on toxicity. In contrast to our results, phosphation increases toxicity to benthic crustaceans and fibroblasts.[21,23] We speculate that this difference can be generated by different preparation methods. Previous studies pre-synthesized phosphate ZnO NPs and exposed them in test media in the presence of phosphate. It seems that pre-synthesized ZnO NPs reacted with phosphate are not efficient to inhibit the release of zinc ions and the presence of other ions could also influence it. Additional toxicity testing of different species with the same transformed ZnO NPs is helpful to conclude test species-dependent toxicity. More research, especially on phosphation and Zn–FeOOH, is necessary to gain a better understanding of the effects of transformation on the toxicity changes of ZnO NPs.

Agglomeration is a well-known factor that reduces the bioavailability and biological toxicity of ENMs.[12,40,41] Therefore, we investigated whether the observed toxicity reduction was attributed to agglomeration caused by transformation. We found that the addition of sulfur, phosphate, and FeOOH resulted in an increased particle size (Table 1); however, the toxicity reduction was not related to particle size changes. For example, greater toxicity was observed with sulfidation at low S/Zn molar ratios than high S/Zn molar ratios, although the hydrodynamic diameters were bigger. In Zn–FeOOH, hydrodynamic diameters varied with different Fe/Zn molar ratios, but toxicity was not affected. Therefore, it is evident that agglomeration did not contribute greatly to the toxicity reduction of the transformed ZnO NPs.

Effect of zinc ions on the toxicity of the transformed ZnO NPs

To explore the mechanism underlying the observed toxicity reduction of the transformed ZnO NPs, we analyzed the quantity of zinc ions present in the bulk solutions. Additionally, we investigated the influence of zinc ions on biological responses. First, we confirmed that zinc ions were released from the pristine ZnO NPs into the bulk solution. Approximately 43 mg L^{-1} of zinc ions were measured in the 50 mg L^{-1} pristine ZnO NPs, and the concentration was maintained over 120 h (Fig. S1G†). The rapid dissolution of zinc is consistent across studies; however, the quantity of released zinc varies. About 90% dissolution of zinc we observed is similar to a previous study reporting close to 100% dissolution from 22.4 nm ZnO NPs,[21] but far greater than other studies that report 13% (0.038 mM from 20 mg L^{-1} 30 nm ZnO NPs)[16] and 1.6% from 40 nm ZnO NPs.[17] These differences suggest that the dissolution of zinc is affected by the type of ZnO NPs (*i.e.*, powder or solution), the synthesis method, the ionic composition of given media, storage conditions, and physicochemical properties such as surface coating and size. The zinc concentration decreased

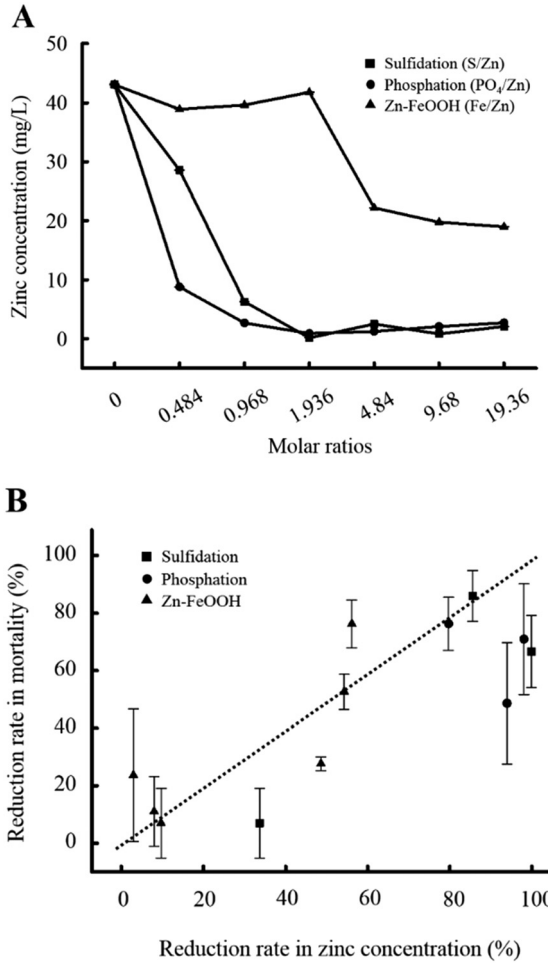

Fig. 5 (A) Zinc concentrations in bulk solutions of the three kinds of transformed zinc oxide nanoparticles (ZnO NPs). (B) The correlation between the toxicity reduction rate and zinc concentration reduction rate. The dotted line represents the equivalent line and the values are presented as mean ± standard deviation (SD).

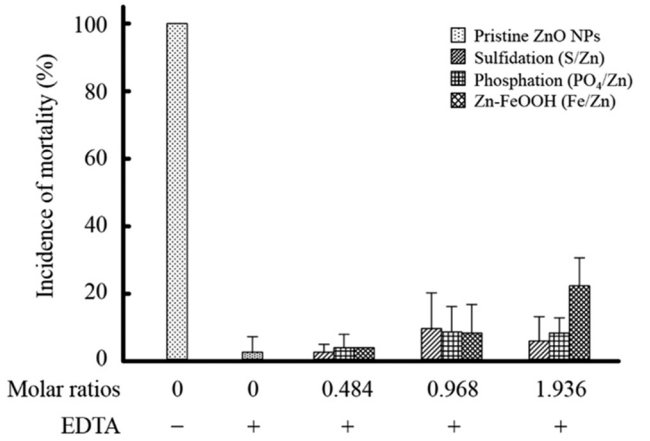

Fig. 6 The percent incidence of embryonic mortality of the three kinds of transformed zinc oxide nanoparticles (ZnO NPs) in different molar ratios after ethylenediaminetetraacetic acid (EDTA) was added. Toxicity of 50 mg L^{-1} pristine ZnO NPs before and after EDTA addition was compared. The values are presented as mean ± standard deviation (SD).

with increasing molar ratios among all three transformations (Fig. 5A). However, the degree of decline was dependent on the type of transformation. Notably, we found that the degree of toxicity reduction correlated well with the degree of zinc concentration reduction measured in the bulk solutions (Fig. 5B). With phosphation, the zinc concentration was reduced by approximately 80% even at the lowest molar ratio of 0.484 at which a significant reduction in toxicity was also observed. The zinc reduction was much higher than that occurred with sulfidation (30%) at the same molar ratio. Similarly, toxicity was significantly reduced by sulfidation in a molar ratio of 0.968 S/Zn at which the zinc concentration was accordingly reduced. Furthermore, when Zn–FeOOH was formed, a noticeable reduction in zinc concentration was observed from 4.84 Fe/Zn, at which toxicity began to decrease. A significant toxicity reduction was observed at 9.68 and 19.36 Fe/Zn, which was twenty times higher than that at 0.484 Fe/Zn. Collectively, these results demonstrate that the toxicity of the transformed ZnO NPs is dependent on the remaining concentration of zinc in the bulk solutions.

To confirm the effect of zinc ions on toxicity, we repeated embryonic toxicity testing after adding EDTA, a potent heavy metal-chelating agent, to each of the transformed ZnO NPs to eliminate the remaining zinc ions in the bulk solutions. As expected, the toxicity of the pristine ZnO NPs significantly decreased (Fig. 6), indicating that zinc ions govern the toxicity of the pristine ZnO NPs, which is consistent with previous studies.[42–44] Notably, the degree of toxicity reduction after adding EDTA was greater than the first observed toxicity reduction upon exposure to three types of transformed ZnO NPs. After adding EDTA, the toxicity was completely reduced to the control level at all molar ratios, regardless of the transformation type. Moreover, there was no difference in toxicity among the three kinds of transformed ZnO NPs after adding EDTA. These observations support the conclusion that the toxicity changes observed with the transformation of ZnO NPs result from the variation in zinc concentrations in the bulk solutions.

We interpreted the reduction in zinc concentration that varied with the type of transformation along with characterization results. The surface composition and morphology changed with sulfidation, which suggests that three types of sulfides, 1) exchanged sulfides with oxygen on the surface, 2) ZnS formed through sulfidation, and 3) remaining sulfides in the bulk solution, are complexed with zinc ions and inhibit the release of zinc ions, resulting in the decrease of zinc ion concentration.[16,32] During phosphation, phosphate ions are known to rapidly degrade ZnO NPs,[18] and similar to sulfide ions, they are complexed with released zinc ions and inhibit the release of zinc ions. We evaluated the embryotic toxicity of the solutions in which sulfur, phosphate, and hydrous ferric oxide were added to $ZnCl_2$, not to ZnO NPs. Lower toxicity was observed when sulfur ions

were added to $ZnCl_2$ compared to phosphate ions at equal low molar ratios (0.484 S/Zn and PO_4/Zn), indicating that the complexation between zinc and sulfide ions is greater than that between zinc and phosphate ions (Fig. S4†). In addition, zinc has a greater binding ability for sulfides compared to phosphates, which further supports this observation.[45] Thus, phosphate ions that rapidly enclose ZnO NPs hinder the release of zinc ions rather than complexation, resulting in a lower concentration of zinc ions in the bulk solution and lower toxicity compared to sulfidation at equivalent low molar ratios. In contrast, the concentration of zinc ions in Zn–FeOOH was maintained at levels similar to that in the pristine ZnO NPs up to a molar ratio of 1.936 Fe/Zn, indicating that the association of FeOOH with ZnO NPs does not affect the release of zinc ions and is less effective to complex zinc ions than sulfidation. From the low efficiency of Zn–FeOOH in reducing zinc ions, we can assume that the reactivity with zinc ions relies on adsorption *via* the formation of an inner-sphere surface complex.[24,46] No significant changes in chemical composition and morphology were observed in the XRD and TEM characterization results. Indeed, FeOOH is commonly applied as an absorbent in WWTPs.[47]

Conclusions

This study demonstrates that the characteristics of ZnO NPs, such as surface composition and morphology, were affected by transformations, subsequently controlling the ability of transformed ZnO NPs to complex with zinc ions. The interference with the release of zinc ions, depending on the type of transformation, consequently determines the biological toxicity of the transformed ZnO NPs.

Author contributions

Gyudong Lee: investigation, and writing – original draft; Byongcheun Lee: investigation, and resource; Ki-Tae Kim: supervision, project administration, writing – original draft, and writing – review & editing.

Conflicts of interest

The authors declare no competing financial interest.

Acknowledgements

This study was supported by the Advanced Research Project funded by the SeoulTech (Seoul National University of Science and Technology).

References

1 A. Kolodziejczak-Radzimska and T. Jesionowski, Zinc oxide-From synthesis to application: A review, *Materials*, 2014, **7**, 2833–2881, DOI: 10.3390/ma7042833.
2 Z. L. Wang and J. Song, Piezoelectric nanogenerators based on zinc oxide nanowire arrays, *Science*, 2006, **312**, 242–246, DOI: 10.1126/science.1124005.
3 C. Kuo, C. Wang, H. Ko, W. Hwang, K. Chang, W. Li, H. Huang, Y. Chang and M. Wang, Synthesis of zinc oxide nanocrystalline powders for cosmetic applications, *Ceram. Int.*, 2010, **36**, 693–698, DOI: 10.1016/j.ceramint.2009.10.011.
4 P. K. Mishra, H. Mishra, A. Ekielski, S. Talegaonkar and B. Vaidya, Zinc oxide nanoparticles: a promising nanomaterial for biomedical applications, *Drug Discovery Today*, 2017, **22**, 1825–1834, DOI: 10.1016/j.drudis.2017.08.006.
5 Y. Zhang, Y. R. Nayak, H. Hong and W. Cai, Biomedical application of zinc oxide nanomaterials, *Curr. Mol. Med.*, 2013, **13**(1), 1633–1645, DOI: 10.2174/1566524013666131111130058.
6 C. Coll, D. Notter, F. Gottshalk, T. Sun, C. Som and B. Nowack, Probabilistic environmental risk assessment of five nanomaterials (nano-TiO_2, nano-Ag, nano-ZnO, CNT, and fullerenes), *Nanotoxicology*, 2015, 1–9, DOI: 10.3109/17435390.2015.1073812Early Online.
7 F. Wu, B. J. Harper and S. L. Harper, Comparative dissolution, uptake, and toxicity of zinc oxide particles in individual aquatic species and mixed populations, *Environ. Toxicol. Chem.*, 2019, **38**, 591–602, DOI: 10.1002/etc.4349.
8 A. J. Miao, X. Y. Zhang, Z. Luo, C. S. Chen, W. C. Chin, H. S. Santschi and A. Quigg, Zinc oxide-engineered nanoparticles: dissolution and toxicity to marine phytoplankton, *Environ. Toxicol. Chem.*, 2010, **29**, 2814–2822, DOI: 10.1002/etc.340.
9 S. Lopes, F. Riberio, J. Wojnarowicz, W. Lojkowski, K. Jurkschat, A. Crossley, A. M. V. M. Soares and S. Lourerio, Zinc oxide nanoparticles toxicity to daphnia magna: size-dependent effects and dissolution, *Environ. Toxicol. Chem.*, 2014, **33**, 190–198, DOI: 10.1002/etc2413.
10 G. V. Lowry, K. B. Gregory, S. C. Apte and J. R. Lead, Transformations of nanomaterials in the environment, *Environ. Sci. Technol.*, 2012, **46**, 6893–6899, DOI: 10.1021/es300839e.
11 J. Zhang, W. Guo, Q. Li, Z. Wang and S. Liu, The effects and the potential mechanism of environmental transformation of metal nanoparticles on their toxicity in organisms, *Environ. Sci.: Nano*, 2018, **5**, 2482, DOI: 10.1039/c8en00688a.
12 G. V. Lowry and E. A. Casman, *Nanomaterial transport, transformation, and fate in the environment, Nanomaterials: Risks and benefits*, 2009, pp. 125–137, DOI: 10.1007/978-1-4020-9491-0_9.
13 R. Ma, C. Levard, J. D. Judy, J. M. Unrine, M. Durenkamp, B. Martin, B. Jefferson and G. V. Lowry, Fate of zinc oxide and silver nanoparticles in a pilot wastewater treatment plant and in processed biosolids, *Environ. Sci. Technol.*, 2014, **48**, 104–112, DOI: 10.1021/es403646x.
14 M. L. Bars, S. Legros, C. Levard, P. Chaurand, M. Tella, M. Rovezzi, P. Browne, J. Rose and E. Doelsch, Drastic change in zinc speciation during anaerobic digestion and composting: instability of nanosized zinc sulfide, *Environ. Sci. Technol.*, 2018, **52**, 12987–12996, DOI: 10.1021/acs.est.8b02697.
15 E. Lombi, E. Donner, E. Tavakkoli, T. W. Turney, R. Naidu,

B. W. Miller and K. G. Scheckel, Fate of zinc oxide nanoparticles during anaerobic digestion of wastewater and post-treatment processing of sewage sludge, *Environ. Sci. Technol.*, 2012, **46**, 9089–9096, DOI: 10.1021/es301487s.

16 R. Ma, C. Levard, F. M. Michel, G. E. Brown Jr and G. V. Lowry, Sulfidation Mechanism for zinc oxide nanoparticles and the effect of sulfidation on their solubility, *Environ. Sci. Technol.*, 2013, **47**, 2527–2534, DOI: 10.1021/es3035347.

17 J. Lv, S. Zhang, L. Luo, W. Han, J. Zhang, K. Yong and P. Christie, Dissolution and microstructural transformation of ZnO nanoparticles under the influence of phosphate, *Environ. Sci. Technol.*, 2012, **46**, 7215–7221, DOI: 10.1021/es301027a.

18 R. Herrmann, J. Garcia-Garcia and A. Reller, Rapid degradation of zinc oxide nanoparticles by phosphate ions, *Beilstein J. Nanotechnol.*, 2014, **5**, 2007–2015, DOI: 10.3762/bjnano.5.209.

19 D. Starnes, J. Unrine, C. Chen, S. Lichtenberg, C. Starnes, C. Svendsen, P. Kille, J. Morgan, Z. E. Baddar, A. Spear, P. Bertsch, K. C. Chen and O. Tsyusko, Toxicogenomic responses of Caenorhabditis elegans to pristine and transformed zinc oxide nanoparticles, *Environ. Pollut.*, 2019, **247**, 917–926, DOI: 10.1016/j.envpol.2019.01.077.

20 S. Bao, M. Huang, W. Tang and T. Wang, J. Xu and T. Fang, Opposite effects of the earthworm Eisenia fetida on the bioavailability of Zn in soils amended with ZnO and ZnS nanoparticles, *Environ. Pollut.*, 2020, **260**, 114045, DOI: 10.1016/j.envpol.2020.114045.

21 H. C. Poynton, C. Chen, S. L. Alexander, K. M. Major, B. J. Blalock and J. M. Unrine, Enhanced toxicity of environmentally transformed ZnO nanoparticles relative to Zn ions in the epibenthic amphipod Hyalella azteca, *Environ. Sci.: Nano*, 2019, **6**, 325, DOI: 10.1039/c8en00755a.

22 X. Qian, Z. Gu, Q. Tang, A. Hong, J. Filser, V. K. Sharma and L. Li, Sulfidation of sea urchin-like zinc oxide nanospheres: Kinetics, mechanisms, and impacts on growth of Escherichia coli, *Sci. Total Environ.*, 2020, 140415, DOI: 10.1016/j.scitotenv.2020.140415.

23 W. N. Everett, C. Chern, D. Sun, R. E. McMahon, X. Zhang, W. A. Chen, M. S. Hahn and H. J. Sue, Phosphate-enhanced cytotoxicity of zinc oxide nanoparticles and agglomerates, *Toxicol. Lett.*, 2014, 177–184, DOI: 10.1016/j.toxlet.2013.12.005.

24 M. L. Schlegel, A. Manceau and L. Charlet, EXAFS study of Zn and ZnEDTA sorption at the goethite (α-FeOOH)/water interface, *J. Phys. IV France*, 1997, **7**, 823–824, DOI: 10.1051/jp4:1997248.

25 E. Haque and A. C. Ward, Zebrafish as a model to evaluate nanoparticle toxicity, *Nanomaterials*, 2018, **8**, 561, DOI: 10.3390/nano8070561.

26 L. C. Wehmas, C. Anders, J. Chess, A. Punnoose, C. B. Pereira, J. A. Greenwood and R. L. Tanguay, Comparative metal oxide nanoparticle toxicity using embryonic zebrafish, *Toxicol. Rep.*, 2015, 702–715, DOI: 10.1016/j.toxrep.2015.03.015.

27 P. V. Asharani, Y. Lianwu, Z. Gong and S. Valiyaveettil, Comparison of the toxicity of silver, gold and platinum nanoparticles in developing zebrafish embryos, *Nanotoxicology*, 2010, 1–12, DOI: 10.3109/17435390.2010.489207Early online.

28 K. T. Kim, L. Truong, L. Wehmas and R. L. Tanguay, Silver nanoparticle toxicity in the embryonic zebrafish is governed by particle dispersion and ionic environment, *Nanotechnology*, 2013, **24**, 115101, DOI: 10.1088/0857-4484/24/11/115101.

29 E. Matijevic and P. Scheiner, Ferric hydrous sols: III. Preparation of uniform particles by hydrolysis of Fe(III)-chloride, –nitrate, and -perchlorate solutions, *J. Colloid Interface Sci.*, 1978, **63**(3), 509–524, DOI: 10.1016/S0021-9797(78)80011-3.

30 C. M. Tran and K. T. Kim, miR-137 and miR-141 regulate tail defects in zebrafish embryos caused by triphenyl phosphate (TPHP), *Environ. Pollut.*, 2020, **262**, 114286, DOI: 10.1016/j.envpol.2020.114286.

31 T. Zhai, Z. Gu, Y. Ma, W. Yang, L. Zhao and J. Yao, Synthesis of ordered ZnS nanotubes by MOCVD-template method, *Mater. Chem. Phys.*, 2006, **100**, 281–284, DOI: 10.1016/j.matchemphys.2005.12.044.

32 P. Banerjee and P. K. Jain, Mechanism of sulfidation of small zinc oxide nanoparticles, *RSC Adv.*, 2018, **8**, 34476, DOI: 10.1039/c8ra06949b.

33 S. Rathnayake, J. M. Unrine, J. Judy, A. F. Miller, W. Rao and P. M. Bertsch, Multitechnique investigation of the pH dependence of phosphate induced transformations of ZnO nanoparticles, *Environ. Sci. Technol.*, 2014, **48**, 4757–4764, DOI: 10.1021/es404544w.

34 K. T. Kim and R. L. Tanguay, The role of chorion on toxicity of silver nanoparticles in the embryonic zebrafish assay, *Environ. Health Toxicol.*, 2014, **29**, e2014021, DOI: 10.5620/eht.e2014021.

35 J. Hua, M. G. Vijver, M. K. Richardson, F. Ahmad and W. J. G. M. Peijnenburg, Particle-specific toxic effects of differently shaped zinc oxide nanoparticles to zebrafish embryos (danio rerio), *Environ. Toxicol. Chem.*, 2014, **33**, 2859–2868, DOI: 10.1002/etc.2758.

36 B. C. Reinsch, C. Levard, Z. Li, R. Ma, A. Wise, K. B. Gregory, G. E. Brown Jr. and G. V. Lowry, Sulfidation of silver nanoparticles decreases Escherichia coli growth inhibition, *Environ. Sci. Technol.*, 2012, **46**, 6992–7000, DOI: 10.1021/es203732x.

37 G. P. Devi, K. B. A. Ahmed, M. K. N. S. Varsha, B. S. Shrijha, K. K. S. Lal, V. Anbazhagan and R. Thiagarajan, Sulfidation of silver nanoparticle reduces its toxicity in zebrafish, *Aquat. Toxicol.*, 2015, **158**, 149–156, DOI: 10.1016/j.aquatox.2014.11.007.

38 D. L. Starnes, J. M. Unrine, C. P. Starnes, B. E. Collin, E. K. Oostveen, R. Ma, G. V. Lowry, P. M. Bertsch and O. V. Tsyusko, Impact of sulfidation on the bioavailability and toxicity of silver nanoparticles to Caenorhabditis elegans, *Environ. Pollut.*, 2015, **196**, 239–246, DOI: 10.1016/j.envpol.2014.10.009.

39 L. Li, L. Hu, Q. Zhou, C. Huang, Y. Wang, C. Sun and G. Jiang, Sulfidation as a natural antidote to metallic nanoparticles ins overestimated: CuO sulfidation yields CuS nanoparticles with increased toxicity in medaka (Oryzias latipes) embryos, *Environ. Sci. Technol.*, 2015, **49**, 2486–2495,

DOI: 10.1021/es505878f.

40 E. Bae, H. J. Park, J. Lee, Y. Kim, J. Yoon, K. Park, K. Choi and J. Yi, Bacterial cytotoxicity of the silver nanoparticle related to physicochemical metrics and agglomeration properties, *Environ. Toxicol. Chem.*, 2010, **29**, 2154–2160, DOI: 10.1002/etc.278.

41 D. Drescher, G. Orts-Gil, G. Laube, K. Natte, R. W. Veh, W. Osterle and J. Kneipp, Toxicity of amorphous silica nanoparticles on eukaryotic cell model is determined by particle agglomeration and serum protein adsorption effects, *Anal. Bioanal. Chem.*, 2011, **400**, 1367–1373, DOI: 10.1007/s00216-011-4893-7.

42 A. Sirelkhatim, S. Mahmud, A. Seeni, N. H. M. Kaus, L. C. Ann, S. K. M. Bakhori, H. Hasan and D. Mohamad, Review on zinc oxide nanoparticles: antibacterial activity and toxicity mechanism, *Nano-Micro Lett.*, 2015, **7**(3), 219–242, DOI: 10.1007/s40820-015-0040-x.

43 H. Ma, P. L. Williams and S. A. Diamond, Ecotoxicity of manufactured ZnO nanoparticles – a review, *Environ. Pollut.*, 2013, **172**, 76–85, DOI: 10.1016/j.envpol.2012.08.011.

44 A. Lvask, K. Juganson, O. Bondarenko, M. Mortimer, A. Villem, K. Kasemets, I. Blinova, M. Heinlaan, V. Slaveykova and A. Kahru, Mechanisms of toxic action of Ag, ZnO and CuO nanoparticles to selected ecotoxicological test organisms and mammalian cells in vitro: a comparative review, *Nanotoxicology*, 2014, **8**(S1), 57–71, DOI: 10.3109/17435390.2013.855831.

45 W. Stumm and J. J. Morgan, *Aquatic chemistry : chemical equilibria and rates in natural waters*, ed. J. L. Schnoor and A. Zehnder, John Wiley & Sons, Inc., New York, 3rd edn., 1996, ch. 6, pp. 325–334.

46 M. Ding, B. H. W. S. De Jong, S. J. Roosendaal and A. Vredenberg, XPS, studies on the electronic structure of bonding between solid and solutes: adsorption of arsenate, chromate, phosphate, Pb^{2+}, and Zn^{2+} ions on amorphous black ferric oxyhydroxide, *Geochim. Cosmochim. Acta*, 2000, **64**(7), 1209–1219, DOI: 10.1016/s0016-7037(99)00386-5.

47 M. Streat, K. Hellgardt and N. L. R. Newton, Hydrous ferric oxide as an adsorbent in water treatment part 1. Preparation and physical characterization, *Process Saf. Environ. Prot.*, 2008, **86**, 1–9, DOI: 10.1016/j.psep.2007.10.007.

